Ultrathin Cellulose Films of Tunable Nanostructured Morphology with a Hydrophobic Component

Laura Nyfors, Miro Suchy, Janne Laine, and Eero Kontturi*

Department of Forest Products Technology, Helsinki University of Technology, P.O. Box 6300, FIN-02015 TKK, Finland

Received January 26, 2009; Revised Manuscript Received February 20, 2009

In recent years, a wide range of different methods to implant nanosized patterns on surfaces have been developed. Spin coating immiscible binary polymer blends is a straightforward method to prepare micro- and nanostructures on thin films. This study utilizes binary blends to effortlessly prepare stable, surface-functionalized cellulose films. Blends of trimethylsilyl cellulose (TMSC) majority phase and polystyrene (PS) minority phase in toluene were spin coated into an ultrathin film, and TMSC was hydrolyzed to cellulose. The films were characterized and quantified using atomic force microscopy (AFM), X-ray photoelectron spectroscopy (XPS), contact angle measurements, and quartz crystal microbalance (QCM-D). AFM revealed that horizontally phase-separated structures form during spin coating: after the hydrolyzation of TMSC to cellulose, PS protrudes from cellulose as distinct patches. The patches are disk-like structures with a circular radial cross-section and a height of ca. 5−20 nanometers. The smaller the amount of PS in the original spin coating solution, the smaller the PS island dimensions in the films. The results obtained from the XPS measurements support the AFM results. Water contact angle of the PS/cellulose films increases from 61° to 71° when the relative amount of hydrophobic PS is increased from 1:100 to 1:5. Thus by simply varying the ratio of the film components subtly tailored hydrophobic properties can be achieved. The swelling of the films due to exposure to water was studied by QCM-D. The swelling was not affected by the amount of PS in the blend, and at equivalent cellulose content the blends and pure cellulose films exhibited similar swelling characteristics. In addition, the QCM-D evaluation demonstrated that the films are stable over extended periods of time and are suitable for fundamental studies by QCM-D.

1. Introduction

Implanting various nano- and microscale features on ultrathin polymeric films is a challenge in the contemporary field of nanoscience.[1] The methods to fulfill this task are roughly categorized into "top-down" techniques (advanced photolithography,[2] laser scanning,[3] nanoimprint lithography,[4] block copolymer lithography,[5] nanocontact printing and writing,[6] dip-pen lithography,[7] and molding[8]) and "bottom-up" techniques (layer-by-layer deposition,[9] surface instabilities,[10,11] patterns with block-copolymers[12] and DNA self-assembly[13]) to name but a few. To benefit from the advantages of both approaches some hybrid techniques have been developed.[14,15] One of the most effortless ("bottom-up") ways to prepare nanostructures on polymer films is to use the simple spin coating process for binary polymer blend solutions. The surface patterns in these films emerge from the complex interplay between the two polymer components, the solvent and the substrate and they are facilitated by the thermodynamic instability driven by spin coating.[16−18] The purpose of this work is to introduce a method to prepare quantitatively reproducible cellulose films of tunable chemical functionality, which is achieved by blending trimethylsilyl cellulose (TMSC) with small amounts of polystyrene (PS) and spin coating the mixture into an ultrathin film.

Ultrathin films from spin-coated polymer blend solutions have been utilized in, for example, antireflective coatings[19] and conductive polymer films.[20] Aside the material applications, polymer blend films also offer an attractive platform for fundamental research.[16,21] In fact, the phase separation of the two polymers during the rapid quench of solvent evaporation in spin coating is still not fully understood.[18]

Scheme 1. Synthesis of Cellulose to TMSC with Hexamethyldisilazane (HMDS) and Subsequent Hydrolysis Back to Cellulose with Gaseous Hydrochloric Acid (HCl)

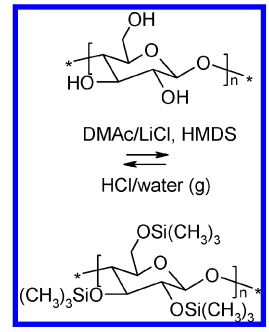

Cellulose, the most abundant biopolymer,[22] has been subject to thin polymer blend films very little, possibly due to its limited solubility.[23,24] Few accounts of thin polymer blend films from more soluble cellulose derivatives exist.[25,26] There is, however, an increasing interest toward cellulose films, both as model substrates for fundamental research and from the material perspective.[22,27] Surface functionalization of cellulosic materials in general and cellulose films in particular is often a laborious undertaking, owing to the often counterintuitive response of cellulose to covalent modifications.[22] In this study, we want to demonstrate how cellulose films with nanosized PS domains can be obtained by the use of TMSC/PS blends and subsequent hydrolysis of TMSC to cellulose (Scheme 1).[28] Normally, the phase separation in the formation of polymer blend films leads to micron scale domains, which is also the case in previously

* Corresponding author. Telephone: +358 9 451 4250. Fax: +358 9 4514 259. E-mail: eero.kontturi@tkk.fi.

10.1021/bm900099e CCC: $40.75
Published on Web 04/01/2009

published TMSC/PS blend films.[26] By simply tuning the ratio of the components, however, nanosized features emerge when the substrate, the polymers, and the solvent are chosen correctly.[17] When PS is applied as the minority phase, tuning the PS concentration results in a series of cellulose films with PS domains of controllable sizes. Since one component is hydrophilic (cellulose) and the other hydrophobic (PS), finely tunable hydrophobic properties are intrinsically linked to the preparation of these films. In other words, this study presents a method to quantitatively modify the surface chemistry of ultrathin cellulose films in a single step during the film preparation.

2. Experimental Section

Materials. TMSC was synthesized from Cellulose from spruce (Fluka) as described previously.[28] The final product was characterized with photoacoustic Fourier transform infrared (FTIR). PS (Aldrich) had a molecular weight of 280 000 Da according to the manufacturer. Formamide (Sigma-Aldrich), ethylene glycol (Riedel-de Haën), and water were used as probe liquids in contact angle measurements. All other chemicals were of analytical grade, and water used was of ultra high quality purified with Millipore Direct-Q 3UV (Millipore, Molsheim, France). Untreated silicon wafers (Si 100 with native oxide layer on top, Okmetic, Espoo, Finland) cut to ca. 1×1 cm^2 squares were used as substrates.

Spin Coating. Ultrathin films of TMSC and PS blends were prepared with spin coating. TMSC and PS were dissolved into toluene both with a solution concentration of 10 g/dm^3. Blends were prepared by mixing the two 10 g/dm^3 solutions and diluting the rest with toluene in a way that the TMSC concentration was always 5 g/dm^3 and PS concentration varied according to the PS/TMSC ratio. The spin coater used was WS-400B-6NPP/LITE (Laurell Technologies Corporation, North Wales, PA, USA). Prior to spin coating, substrates were rinsed twice with toluene (4000 rpm for 15 s). Spin coating was performed with the spinning speed of 4000 rpm and with the acceleration speed of 2130 rpm/s. The deposition of the blend solution was performed on a static substrate, and the spinning was retained ca. 30 s after the disappearance of the Newtonian rings which took place a few seconds after the acceleration. The TMCS film for quartz crystal microbalance (QCM-D) studies was prepared from 5 g/L solution to obtain the same amount of cellulose as in the blends. The spin-coated surfaces containing TMSC were hydrolyzed in a 10 wt % aqueous HCl vapor environment for 2 min. During the hydrolysis, the spin-coated TMSC is converted back to cellulose (Scheme 1).

Atomic Force Microscopy (AFM). Model surface morphology and layer thickness was determined using a Nanoscope IIIa Multimode scanning probe microscope (Digital Instruments, Inc., Santa Barbara, CA). The images were scanned in tapping mode using a J-scanner and silicon cantilevers (NSC15/AIBS from Ultrasharp μmasch, Tallinn, Estonia). The radius of curvature for the tip according the manufacturer was less than 10 nm, and typical resonance frequency of the cantilever was 325 kHz. Two parallel surfaces were prepared, and at least two points on each was imaged. No image processing except flattening was performed. Film thicknesses were studied by scratching the samples with a needle and determining the height difference between the revealed substrate and the intact areas of the film. All quantitative data was extracted from the height images.

Image Analysis. Image analysis was performed using Nanoscope softwares (versions V5.30 R3SR3 and V6.13 R1, Digital Instruments, Inc.) and Scanning Probe Image Processor (SPIP) software (version 4.5.3, Image Metrology, Lyngby, Denmark). The coverage of PS was determined using the Grain Analysis module in SPIP with Threshold algorithm. Each value is an average of three images.

X-ray Photoelectron Spectroscopy (XPS). Chemistry of the model surfaces was studied with XPS. XPS measurements were performed with an AXIS 165 (Kratos Analytical, Manchester, UK) spectrometer using a monochromated Al Kα X-ray source. All samples were pre-evacuated overnight to stabilize ultrahigh vacuum (UHV) conditions. UHV condition was monitored during the whole measurement. Two parallel samples were prepared, and each sample was analyzed at three points. Elemental surface composition was determined from low-resolution scans recorded with 80 eV pass energy and 1 eV steps. Carbon 1s and oxygen 1s high-resolution spectra were determined using 20 eV pass energy at 0.1 eV steps. The carbon 1s emission was resolved into various contributions corresponding to distinct chemical states of carbon according to literature.[29]

Contact Angle Measurements. Contact angle measurements were performed to acquire information of the changing hydrophobicity of the surfaces. A CAM-200 contact angle goniometer (KSV Instruments Ltd., Helsinki, Finland) was used to determine equilibrium advancing contact angles of water, ethylene glycol and formamide on the model surfaces. The measurements were conducted in ambient air at room temperature. The size of the drop was 7 μL with all the measured probe liquids. At least five measurements from two different surfaces per test point were performed. Contact angle calculations were performed with CAM-200 software (KSV Instruments Ltd., Helsinki, Finland). The calculations are based on a numerical solution of the full Young−Laplace equation.

Quartz Crystal Microbalance. Studies on swelling and stability of the films were performed with a Q-Sense E4 instrument (Q-Sense AB, Gothenburg, Sweden). The hydrolyzed crystals were rinsed with water and thoroughly dried with nitrogen before being mounted in the measuring chamber. Right after starting the measurement, the pump was turned on at high speed (0.8 mL/min) until the measuring chamber was filled with water. Then the water flow was lowered to 0.1 mL/min, continued for 120 min, and then the pump was turned off. The total time of each measurement was at least 15 h. All measurements were recorded at 5 MHz fundamental resonance frequency and its overtones 15, 25, 35, 55, and 75 MHz. The third overtone (15 MHz) was used in the evaluation of the data. The temperature was stabilized to 25 °C, and each experiment was repeated at least two times.

3. Results and Discussion

3.1. Qualitative Morphology. Representative 5×5 μm^2 AFM height images of unhydrolyzed PS/TMSC films and hydrolyzed PS/cellulose films are presented in Figure 1. It shows the laterally phase-separated nanosized structure that forms during the rapid quench of spin coating procedure. Thin films spin coated from immiscible polymer blend solution form regular patterns due to constraints caused by the interfaces.[21,30] The final film morphology in spin-coated polymer blend films is a result of consecutive phase separation and dewetting. As spin coating commences, PS and TMSC form a vertically phase-separated structure. TMSC has higher affinity to hydrophilic SiO_x substrate, and thus PS forms a layer on the polymer blend−air interface. The upper PS layer is broken as a result of dewetting, and the holes formed are then filled by the TMSC from the lower layer, a theory put forward for blend films in general.[18] Commonly, the lateral phase separation in ultrathin polymer blend films results in micrometer sized phase domains.[16,17,19,26,31,32] When the initial PS concentration is small enough, however, the subsequent upper PS layer coalesces into nanosized droplets of disk-like shape[33−36] that are visible in Figure 1.

The occurrence of dewetting as the original reason behind the morphology in the films of Figure 1 can be effortlessly confirmed by annealing the films over the glass transition temperature (T_g) of PS.[18,35] When films are heated above T_g, and kept in the oven for 24 h, no additional dewetting should occur.[18] An AFM height image of the film after 24 h of annealing is shown in the Supporting Information (Figure S1).

PS/TMSC films in Figure 1 are rather smooth (root-mean-square (rms) roughness ~0.5 nm in 10×10 μm^2 scan areas),

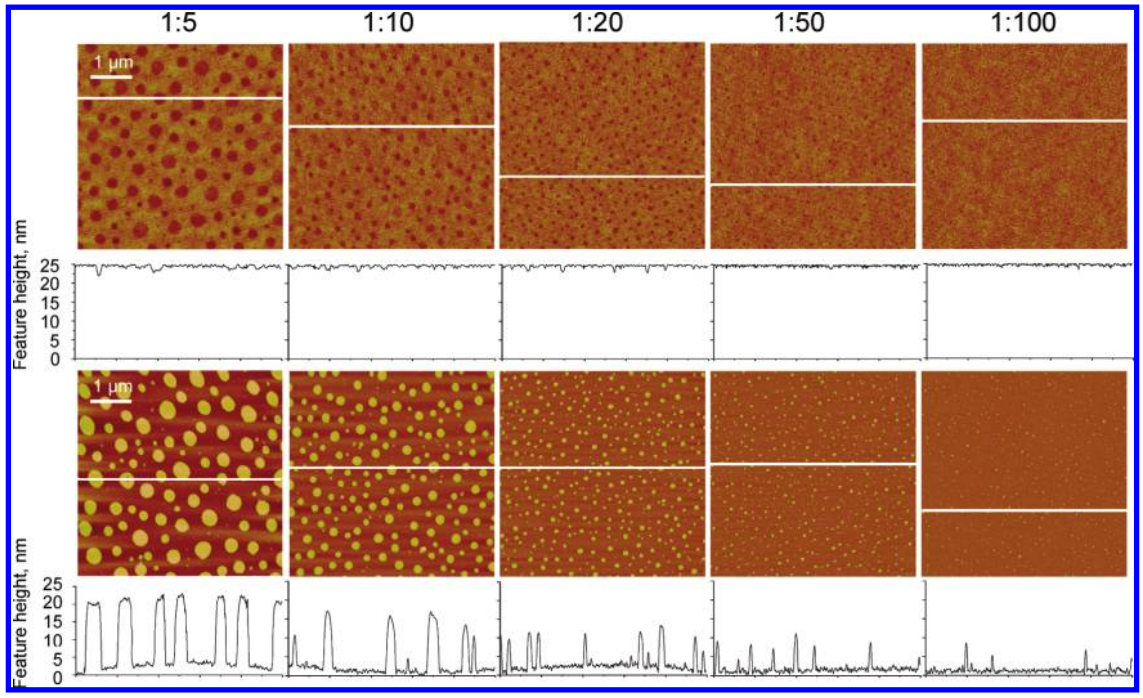

Figure 1. AFM height images and typical height profiles of the blend films, 5 × 5 μm^2 scans: PS/TMSC films on the top row and PS/cellulose films on the bottom row. White line indicates the place where the height profile is taken. In the height image, light areas are higher and dark areas are lower. The height scale is 10 nm in all the PS/TMSC images and 40 nm in all the PS/cellulose images.

Scheme 2. Cross-sectional Representation of the Blend Films[a]

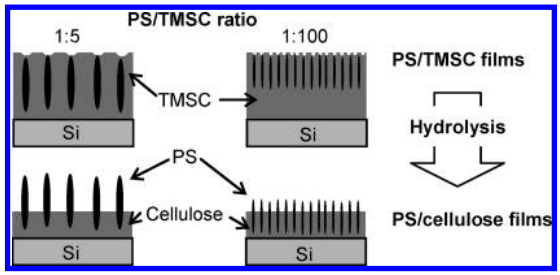

[a] On the top row there are PS/TMSC films: ratio 1:5 on the left and ratio 1:100 on the right. On the bottom row there are the same films but now TMSC is hydrolyzed to cellulose. The dimensions are not to scale (the vertical direction is grossly exaggerated compared to the horizontal one).

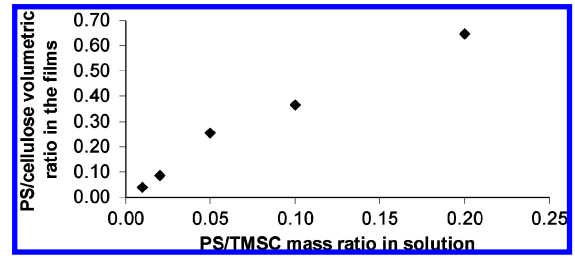

Figure 2. Correlation between the volumetric ratio of PS and cellulose in the films and the mass ratio of PS and TMSC in the original spin coating solution. The volume is calculated from the quantitative information obtained from the AFM height images.

but when TMSC is hydrolyzed to cellulose (Scheme 1), distinct island-like PS domains protruding from cellulose background are revealed (rms roughness varying between 6 nm for PS/cellulose 1:5 and 1 nm for PS/cellulose 1:100 in 10 × 10 μm^2 scan areas). Similar films and the fundamentals of the morphology formation were recently studied by Kontturi et al.,[26] only with a larger share of PS.

The disk-like shape with a circular radial cross-section of PS domains in Figure 1 is precisely the reason why PS was selected as the hydrophobic blend component with TMSC. Many other polymers, which can be dissolved with TMSC, do not form such distinct features on ultrathin blend films. The disk-like shape and the circular radial cross-section of PS domains originate from its considerable immiscibility and surface tension difference with TMSC, which is also responsible for the convex shape of the PS discs on the TMSC interface (Scheme 2).[17] By hydrolyzing TMSC to cellulose, we are able to obtain ultrathin cellulose films with conspicuous PS domains, which are easy to quantify.

3.2. Quantitative Morphology. The volume of each component in the PS/cellulose film can be calculated from the AFM height images when the film thickness, the PS coverage, and the PS domain height are known. In order to determine the total height of PS domains, PS is selectively dissolved with toluene from the PS/cellulose films. The dissolution yields nanoporous cellulose thin films whose AFM height images used in the calculations are shown in the Supporting Information (Figure S2). The horizontal distortion caused by AFM tip exaggeration is eliminated in the PS domain size determination by taking the average value after the hydrolysis of TMSC to cellulose and after the selective dissolution of PS. The linear correlation between PS/cellulose ratio in the films and PS/TMSC ratio in the original spin coating solution is presented in Figure 2. The difference between the PS/cellulose ratio in the films and the PS/TMSC ratio in the original spin coating solution is that the PS/cellulose ratio is volumetric and the PS/TMSC is mass ratio. TMSC hydrolysis to cellulose has an effect as well. All calculations are expressed in detail in the Supporting Information.

PS/TMSC ratios in the films were calculated by using the density of amorphous cellulose (1.48),[37] the density of PS (1.06)[38] and the degree of substitution (DS) of TMSC calculated from XPS measurements. The DS of TMSC is 2.2, which means that 2.2 of the three hydroxyl groups in the repeating unit of cellulose are replaced by trimethylsilyl groups. In Table 1, the calculated values of PS/TMSC mass ratios in films are compared

Table 1. A Comparison of the PS/TMSC Mass Ratios in the Original Spin Coating Solutions and the Calculated Correspondent PS/TMSC Mass Ratios in the Films

PS/TMSC mass ratio in solution	PS/TMSC mass ratio in films
0.2	0.2
0.1	0.1
0.05	0.09
0.02	0.03
0.01	0.01

to PS/TMSC mass ratios in the original spin coating solution. The correlation is linear, and the calculated PS/TMSC ratios in the films are largely congruent with the initial ratios. The discrepancy in Table 1 with the original 0.05 PS/TMSC ratio and its corresponding ratio, observed by AFM in the film (0.09), reveals that the initial mass ratios in a polymer blend solution do not necessarily always result in exact matches in the subsequent films after spin coating. However, the data in Figure 2 and Table 1 indicate that the initial PS/TMSC ratio can be used to linearly tune the PS ratio in the cellulose/PS films.

Further quantification of the PS/cellulose ratio in the films was performed by XPS (Figure 3). Carbon bonded merely to hydrogen is present only in PS. Thus the origin of the C−H bonds in the films is mainly due to PS, although some hydrocarbon impurities are always present. In Figure 3, the percentage of C−H bond emission is shown as a function of the concentration of PS in the initial spin coating solution. XPS measurements are in correlation with the AFM results. The higher the ratio of PS in the spin coating solution, the higher the amount of PS in the films. This result is also in concert with other studies of polymer blend thin films.[31,33,35] The slight discrepancy of the XPS data with AFM data (Figure 3) originates from the ambiguity of quantitative XPS analysis, especially if dealing with inhomogeneous materials. The fact that should always be kept in mind is that the requirement for the accurate interpretation is a homogeneous distribution of the components within the sample.

3.3. Tuning the Hydrophobicity. PS is hydrophobic and cellulose is hydrophilic material. When the PS/TMSC, i.e., PS/cellulose ratio, is varied, the hydrophilicity/hydrophobicity of the films can easily be tuned. Equilibrium advancing contact angles with three different probe liquids as a function of the PS/TMSC ratio in the initial spin coating solution are shown in Figure 4. When the amount of hydrophobic PS in the film decreases, the contact angle also decreases. The change from 71° (PS/cellulose 1:5 film) to 61° (PS/cellulose 1:100 film) is subtle but detectable. The polarity of the probe liquids decreases from water to ethylene glycol. Logically, the contact angles decrease in the same order. Water contact angles on thin film

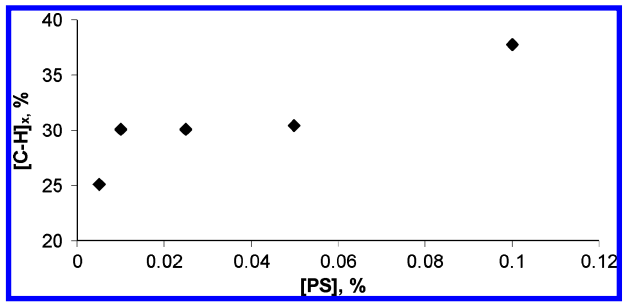

Figure 3. The percentage of carbon $[C-H]_x$ bonds as a function of the PS concentration in the original spin coating solution. The relative amount of the $[C-H]_x$ bonds is obtained from the XPS measurements.

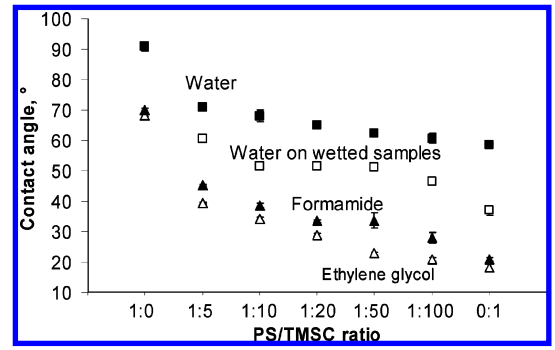

Figure 4. Equilibrium contact angles with water ■, water on wetted samples □, formamide ▲, and ethylene glycol △. Angles are the average, and the error is the standard deviation from all the measured parallel samples.

of pure PS are in accordance with the literature.[39] The case of pure cellulose films is more ambiguous. In the literature, only water contact angles on cellulose from TMSC prepared by Langmuir−Blodgett (LB) technique have been stated.[39−41] They vary from 25° to 45°, while our result is 59°. The difference is due to dissimilarities between the films prepared by spin coating and LB technique. This issue is subject to ongoing studies in our research group,[42] and the results will be published later elsewhere.

Cellulosic materials undergo irreversible changes upon wetting and subsequent drying.[24] Therefore, the effect of wetting and consecutive drying of the films on the water contact angles was studied, and it is shown in Figure 4. The history of the surfaces is quite important: the equilibrium contact angles with water decreased considerably. Also the effect of the PS/TMSC ratio in the original spin coating solution is emphasized. The contact angle of water on pure cellulose regenerated from TMSC decreased approximately 20° after wetting, whereas the contact angle of the blend films decreased approximately 10°.

The decrease in contact angle may seem unexpectedly subtle compared to the rather large differences in PS coverage among the films (Figure 2 and Table S1). Therefore, experimental contact angles were compared to theoretical ones obtained from the Cassie−Baxter equation:[43]

$$\cos\theta_c = \varphi_A \cos\theta_A + \varphi_B \cos\theta_B$$

where θ_c is the contact angle of the blend, φ_A and φ_B are the coverage of the components A and B, and θ_A and θ_B are the contact angles of the pure components. Recently, discussion about the validity and applicability of the Cassie−Baxter equation has emerged.[44,45] However, the majority of researchers agree that when the surface fraction parameter is considered as a global property of the surface rather than a local value, the Cassie−Baxter equation is in line with practice, and it gives a good estimation of the contact angles of the two component surfaces.[45,46] A comparison of the theoretical Cassie−Baxter and experimental contact angles are shown in Figure 5. The experimental contact angles coincide reasonably well with the theoretical ones. The best correlation is found with water.

The tunable hydrophobic character is inherent to the PS/cellulose system, but it is just one example of the potential usage of binary blends to prepare cellulose films with various functionalities. Other hydrophobic polymers bearing different chemical characteristics may be utilized with TMSC to manufacture cellulose films with desired functionalities. This can be

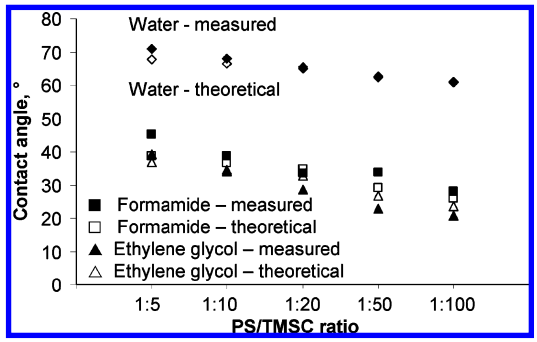

Figure 5. A comparison between measured contact angles and theoretical angles obtained from the Cassie−Baxter equation. Measured contact angles: with water ◆, formamide ■, and ethylene glycol ▲; theoretical angles: with water ◇, formamide □, and ethylene glycol △.

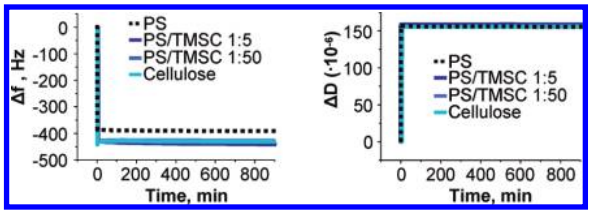

Figure 6. QCM-D frequency (left) and dissipation (right) data comparison of PS, PS/TMSC blends, and pure cellulose. Water is added to the system at $t = 0$ min. The third overtone (15 MHz) only is reported.

achieved without applying complex lithographic techniques or laborious covalent modification of cellulose.

3.4. Swelling and Stability. In addition to well-defined chemical and morphological characterization, stability of the ultrathin films in aqueous environment is essential for their successful use in material applications and fundamental studies. A change of film characteristics or its instability toward solvent exposure can interfere with the actual intended purpose and lead to incorrect observations. Recently, QCM-D has become a popular method for studying adsorption and surface interactions of cellulose and cellulose-based model films.[27] The QCM-D method is based on measuring frequency changes of oscillating crystals, which indicates a change in mass deposited on the crystal. In addition, a change in dissipation that describes changes in viscoelastic/softness properties of the deposited mass is measured simultaneously. The QCM-D technique was used to assess the stability and behavior of the prepared PS/TMSC blend films in aqueous environment over an extended period of time. Representative PS/TMSC blends (1:5 and 1:50) and both individual components as references were evaluated. The study followed a similar concept described previously;[47] however, instead of ethanol-to-water solvent exchange in the measuring chamber, a direct exchange from air to water was implemented. The comparison of frequency and dissipation change of blends, pure cellulose, and PS films after exposure to water are shown in Figure 6.

The frequency and dissipation changed immediately after the film-coated crystals were exposed to water. Compared to pure PS, the frequency drop is more pronounced (approximately 40 Hz) for films containing cellulose due to the water uptake of the cellulose (swelling). The frequency decrease values measured for the blends and pure cellulose were virtually identical. Since the cellulose content in the blends and pure cellulose films is equal, this indicates that the PS present in the blend has no effect on the swelling of the cellulose component in the film. The behavior is expected since PS is present as island-like domains only on the surface of the cellulose films. After the initial drop, the frequencies of the films remain constant over the period of over 15 h. The dissipation measurements showed similar trends. An instant increase simultaneously with the frequency drop was observed for all cellulose-containing films and PS. After the initial increase, the dissipation values remained constant during the time of measurement. In contrast to the frequency measurement, no difference in dissipation was observed between pure PS and the cellulose containing films. The swelling of the cellulose-containing films did not appear to significantly affect the softness of the films. The demonstrated stability of the films during the measurement over an extensive period of time coupled with good reproducibility of the measurements makes these films suitable substrates for fundamental studies of the effect of hydrophobicity on adsorption and interaction of variety of substances. For example, the films offer an unusual template for enzymatic studies: if cellulose-specific enzymes are applied, the substrate contains both specific (cellulose) and nonspecific (PS) adsorption sites. This kind of mixture of specific and nonspecific sites is similar to cases found often in nature.

4. Conclusions

Reproducible ultrathin blend films of PS and cellulose with tunable nanostructured hydrophobic properties were prepared. Hydrophobic functionalization was achieved with an effortless "bottom-up" technique by spin coating a binary blend solution of PS and TMSC, without covalent modification or lithographic complexity. Surface chemistry and morphology of the films was characterized and quantified. Blend films form horizontally phase-separated structures during spin coating due to dewetting. Dimensions of the PS islands depend linearly on the amount of PS in the original spin-coating solution: the smaller the amount of PS in the solution, the smaller the dimensions in the films. By varying the ratio of the film components, tailored hydrophobic properties can be achieved in a simple manner. Hydrophilicity slightly decreases when the amount of hydrophobic PS is increased. The films are stable in the aqueous environment, and the presence of PS in the blends has no effect on swelling characteristics of the films. We foresee that replacing PS with an alternative hydrophobic polymer in the TMSC/PS blend may lead to a method of introducing diverse chemical functionalities on cellulose films.

Acknowledgment. We acknowledge Dr. Leena-Sisko Johansson for recording the XPS data and helping in analyzing the results. E.K. acknowledges the Academy of Finland (No. 129068) for financial support.

Supporting Information Available. Supporting Information includes an AFM image of the blend film annealed for 24 hours (S1), AFM images used in determining film thickness and PS domain size (S2), AFM images of films after selective dissolution of PS (S3), contact angles with three different probe liquids as a function of time (S4), PS coverages in the PS/cellulose films, and explanation of the calculations in Section 3.2. This material is available free of charge via the Internet at http://pubs.acs.org.

References and Notes

(1) del Campo, A.; Arzt, E. *Chem. Rev.* **2008**, *108*, 911–945.
(2) Meisel, D. C.; Wegener, M.; Busch, K. *Phys. Rev. B: Condens. Matter Mater. Phys.* **2004**, *70*, 165104-1–165104-10.

(3) Tormen, M.; Businaro, L.; Altissimo, M.; Romanato, F.; Cabrini, S.; Perennes, F.; Proietti, R.; Sun, H.-B.; Kawata, S.; Di Fabrizio, E. *Microelectron. Eng.* **2004**, *73*−*74*, 535–541.
(4) Chou, S. Y.; Krauss, P. R.; Renstrom, P. J. *J. Vac. Sci. Technol., B* **1996**, *14*, 4129–4133.
(5) Park, M.; Harrison, C.; Chaikin, P. M.; Register, R. A.; Adamson, D. H. *Science* **1997**, *276*, 1401–1404.
(6) Gratson, G. M.; Xu, M.; Lewis, J. A. *Nature (London)* **2004**, *428*, 386.
(7) Piner, R. D.; Zhu, J.; Xu, F.; Hong, S.; Mirkin, C. A. *Science* **1999**, *283*, 661–663.
(8) Schift, H.; Heyderman, L. J.; Auf der Maur, M.; Gobrecht, J. *Nanotechnology* **2001**, *12*, 173–177.
(9) Zhang, C.; Hirt, D. E. *Polymer* **2007**, *48*, 6748–6754.
(10) Weiss, R. A.; Zhai, X.; Dobrynin, A. V. *Langmuir* **2008**, *24*, 5218–5220.
(11) Higgins, A. M.; Jones, R. A. L. *Nature (London)* **2000**, *404*, 476–478.
(12) Segalman, R. A. *Mater Sci. Eng., R* **2005**, *48*, 191–226.
(13) Winfree, E.; Liu, F.; Wenzler, L. A.; Seeman, N. C. *Nature (London)* **1998**, *394*, 539–544.
(14) Wang, D.; Möhwald, H. *J. Mater. Chem.* **2004**, *14*, 459–468.
(15) Lin, C.; Ke, Y.; Liu, Y.; Mertig, M.; Gu, J.; Yan, H. *Angew. Chem., Int. Ed.* **2007**, *46*, 6089–6092.
(16) Budkowski, A. *Adv. Polym. Sci.* **1999**, *148*, 1–111.
(17) Walheim, S.; Böltau, M.; Mlynek, J.; Krausch, G.; Steiner, U. *Macromolecules* **1997**, *30*, 4995–5003.
(18) Heriot, S. Y.; Jones, R. A. L. *Nat. Mater.* **2005**, *4*, 782–786.
(19) Walheim, S.; Schäffer, E.; Mlynek, J.; Steiner, U. *Science* **1999**, *283*, 520–522.
(20) Nardes, A. M.; Kemerink, M.; Janssen, R. A. J.; Bastiaansen, J. A. M.; Kiggen, N. M. M.; Langeveld, B. M. W.; van Breemen, A. J. J. M.; de Kok, M. M. *Adv. Mater.* **2007**, *19*, 1196–1200.
(21) Binder, K. *Adv. Polym. Sci.* **1999**, *138*, 1–89.
(22) Klemm, D.; Heublein, B.; Fink, H.-P.; Bohn, A. *Angew. Chem., Int. Ed.* **2005**, *44*, 3358–3393.
(23) Klemm, D.; Philipp, B.; Heinze, T.; Heinze, U.; Wagenknecht, W. *Comprehensive Cellulose Chemistry, Fundamentals and Analytical Methods*; Wiley-VCH: Chichester, 1998; Vol. 1,Chapter 2.2.
(24) Burchard, W. *Cellulose* **2003**, *10*, 213–225.
(25) Lua, Y.-Y.; Cao, X.; Rohrs, B. R.; Aldrich, D. S. *Langmuir* **2007**, *23*, 4286–4292.
(26) Kontturi, E.; Thüne, P. C.; Niemantsverdriet, J. W. *Macromolecules* **2005**, *38*, 10712–10720.
(27) Kontturi, E.; Tammelin, T.; Österberg, M. *Chem. Soc. Rev.* **2006**, *35*, 1287–1304.
(28) Kontturi, E.; Thüne, P. C.; Niemantsverdriet, J. W. *Langmuir* **2003**, *19*, 5735–5741.
(29) Beamson, G.; Brigg, D. *High-Resolution XPS of Organic Polymers*; John Wiley & Sons: Chichester, 1992.
(30) Jones, R. A. L. *Curr. Opin. Colloid Interface Sci.* **1999**, *4*, 153–158.
(31) Wang, P.; Koberstein, J. T. *Macromolecules* **2004**, *37*, 5671–5681.
(32) Bucknall, D. G. *Prog. Mater. Sci.* **2004**, *49*, 713–786.
(33) Müller-Buschbaum, P.; Gutmann, J. S.; Stamm, M. *Macromolecules* **2000**, *33*, 4886–4895.
(34) Affrossman, S.; O'Neill, S. A.; Stamm, M. *Macromolecules* **1998**, *31*, 6280–6288.
(35) Iyer, K. S.; Luzinov, I. *Langmuir* **2003**, *19*, 118–124.
(36) Ton-That, C.; Shard, A. G.; Teare, D. O. H.; Bradley, R. H. *Polymer* **2001**, *42*, 1121–1129.
(37) Chen, W.; Lickfield, G. C.; Yang, C. Q. *Polymer* **2004**, *45*, 1063–1071.
(38) Weast, R. C., Ed. *CRC Handbook of Chemistry and Physics*, 61st ed.; CRC Press: Boca Raton, 1980; C-740.
(39) Tammelin, T.; Saarinen, T.; Österberg, M.; Laine, J. *Cellulose* **2006**, *13*, 519–535.
(40) Holmberg, M.; Berg, J.; Stemme, S.; Ödberg, L.; Rasmusson, J.; Claesson, P. *J. Colloid Interface Sci.* **1997**, *186*, 369–381.
(41) Schaub, M.; Wenz, G.; Wegner, G.; Stein, A.; Klemm, D. *Adv. Mater.* **1993**, *5*, 919–922.
(42) Kontturi, E.; Osterberg, M.; Lankinen, A. *Abstracts of Papers, 235th ACS National Meeting*, New Orleans, LA, United States, April 6−10, 2008; American Chemical Society: Washington, D.C., 2008.
(43) Cassie, A. B. D. *Discuss. Faraday Soc.* **1948**, *3*, 11–16.
(44) Gao, L.; McCarthy, T. J. *Langmuir* **2007**, *23*, 3762–3765.
(45) Panchagnula, M. V.; Vedantam, S. *Langmuir* **2007**, *23*, 13242.
(46) McHale, G. *Langmuir* **2007**, *23*, 8200–8205.
(47) Fält, S.; Wågberg, L.; Vesterlind, E.-L.; Larsson, P. T. *Cellulose* **2004**, *11*, 151–162.

BM900099E

Supporting Information

for

Ultrathin cellulose films of tunable nanostructures morphology with a hydrophobic component

by

Laura Nyfors, Miro Suchy, Janne Laine, Eero Kontturi

Supporting Information includes atomic force microscopy (AFM) image of the blend film annealed for 24 hours (S1), AFM images used in determining film thickness and PS domain size (S2), AFM images of films after selective dissolution of PS (S3), contact angles with three different probe liquids as a function of time (S4), PS coverages in the PS/cellulose films and explanation of the calculations in Section 3.2 Quantitative morphology.

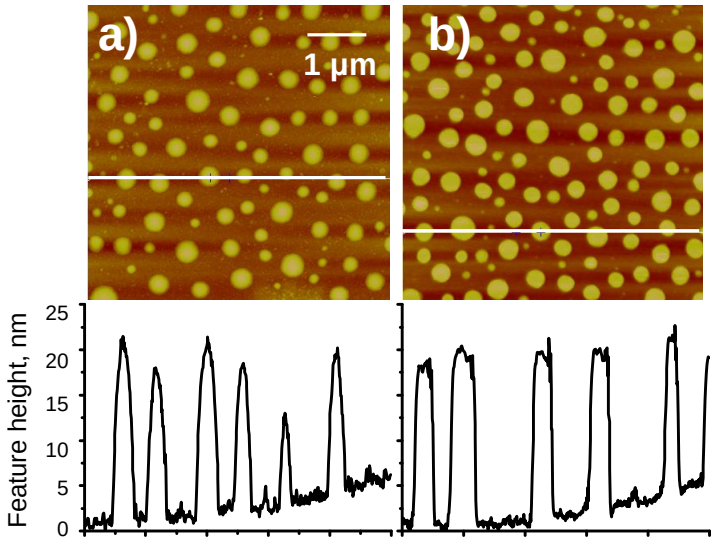

Figure S1. a) 5×5 µm^2 AFM height image and height profile of the PS/cellulose 1:5 film after 24 hours of annealing above Tg of PS and b) 5×5 µm^2 AFM height image and height profile of the PS/cellulose 1:5

film without annealing. Height scale is 50 nm in the both images. The white line indicates the place where the height profile is taken.

S1 Annealing. The occurrence of dewetting as the original reason behind the morphology in the films of can be effortlessly confirmed by annealing the films over the glass transition temperature (T_g) of PS. The PS/cellulose 1:5 film were annealed in 110 °C for 24 hours. No additional dewetting was noticed, only slight softening of the PS domains.

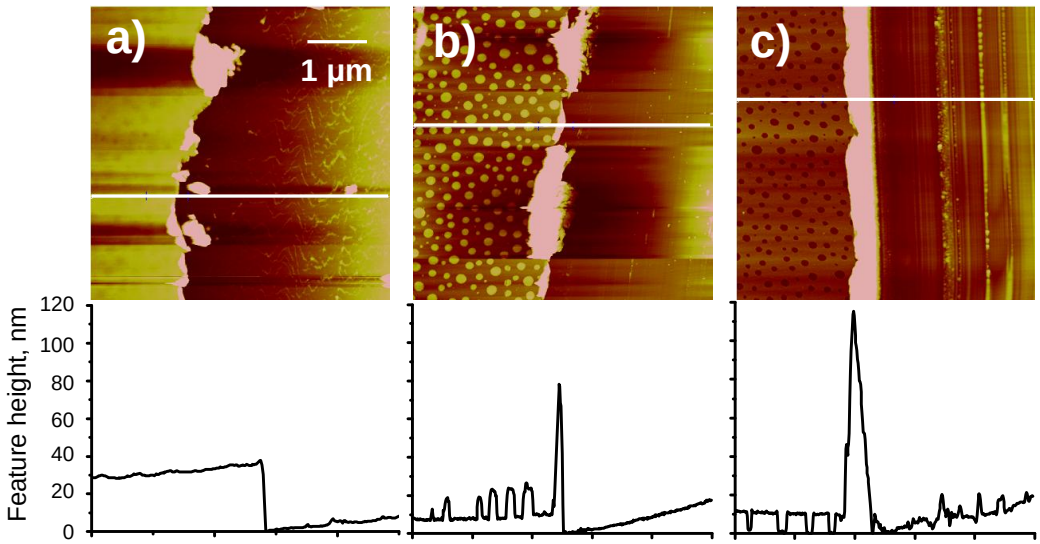

Figure S2. Representative 10×10 µm^2 AFM height images and height profiles of the scratched blend films used to determine film thickness and PS domain dimensions. a) PS/TMSC film b) PS/cellulose film c) Porous cellulose film (PS dissolved selectively from the PS/cellulose film). Height scale is 50 nm in all the images. The white line indicates the place where the height profile is taken.

S2 Film thickness was studied by scratching the samples with a needle and determining the height difference between the revealed substrate and the intact areas of the film. After the hydrolysis of TMSC to cellulose, film thickness decreased from 30 nanometers to 10 nanometers. PS removal did not change the thickness of the film.

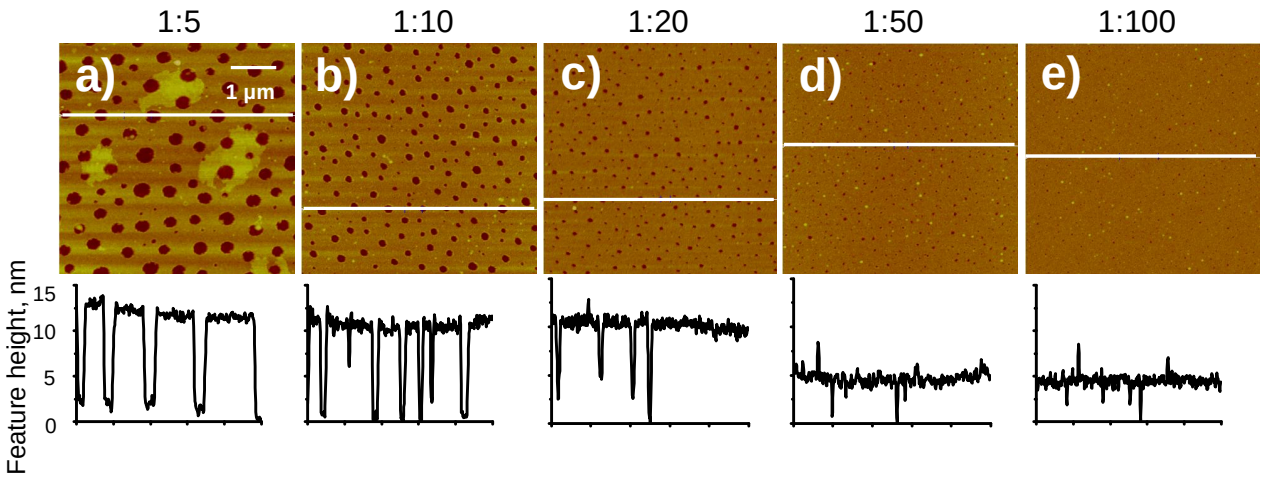

Figure S3. Representative 5×5 µm^2 AFM height images and height profiles of the porous cellulose films (PS/cellulose films where PS has been selectively dissolved). The ratios above images state the PS/TMSC mass ration in the initial spin coating solution a) 1:5, b) 1:10, c) 1:20, d) 1:50 and e) 1:100. Height scale is 30 nm in all the images. The white line indicates the place where the height profile is taken.

S3 Morphology quantification. PS is selectively dissolved by immersing the films in toluene for one hour. The dimensions of the holes left by the PS are determined from the images. The horizontal distortion caused by AFM tip exaggeration is eliminated in the PS domain size determination by taking the average value after the hydrolysis of TMSC to cellulose (Figure 2) and after the selective dissolution of PS (Figure S3).

PS coverages were determined using the Grain Analysis module with Threshold algorithm (Table S1). The coverage stated are averages from the PS coverages in the PS/cellulose films and the coverages left by PS in the cellulose films (PS/cellulose films where PS has been selectively dissolved) to eliminate AFM tip error with small features. The coverage values are used in the calculations explained below.

Table S1. Average PS coverages calculated from the PS/cellulose and cellulose films (coverage of the holes left by PS).

Initial PS/TMSC ratio	PS coverage, %
1:5	21
1:10	15
1:20	12
1:50	6
1:100	3

The volumetric ratios in the PS/cellulose films (Figure 2) were calculated with the help of quantitative information extracted from Figures 1, S2 and S3. The volume of PS per image area was calculated using the PS coverages (Table S1), the heights of the PS patches (Figure 1) and the heights of the holes left by PS after the selective dissolution (Figure S3). The total height of the PS patches was calculates by adding the heights of the PS patches (Figure 1) to the height of the holes left by PS after the selective dissolution (Figure S3). When the total height of the PS patches is multiplied by the PS coverage and the image area, the volume of PS in the PS/cellulose films is obtained. The volume of cellulose per image area was calculated using film thicknesses (Figure S2), PS coverages (Table S1) and the depth of the holes left by PS patches (Figure S3). The volume of the holes left by former PS patches was calculated by multiplying PS coverage with the depth of the holes and the image area. The volume of cellulose was obtained by multiplying the film thickness with the image area and subtracting the volume of the holes left by PS. The volumetric ratios are presented in Figure 2.

The degree of substitution (DS) of the TMSC film can be calculated when the relative amount of C-Si emission is known (obtained from the XPS measurements). Theoretical DS is plotted as a function of the theoretical relative C-Si emission and then according to the experimental relative C-Si emission data DS

of the TMSC is determined. With the help of DS, the molecular weight of the repeating unit of TMSC can be calculated. In this case C-Si relative emission was 52 % which corresponds to DS 2.2.

According to the PS/TMSC mass ratio in the initial spin coating solution the volumetric ratio of PS/cellulose in the hydrolyzed films is obtained from Figure 2. Using volumetric ratio and densities of PS and cellulose, the masses of PS and cellulose in the films can be calculated using:

$m = \rho \times V$,

where m is mass, ρ is density and V is volume.

Masses of PS and cellulose in the films can be converted to molar amount (n=m/M) by using the molar mass of the repeating unit of the polymer.

The molar amount of cellulose in the films is the same as the molar amount of TMSC in the films (Scheme 1). Therefore, the mass of the TMSC in the films can be calculated using the molar mass of TMSC, calculated from DS. The mass ratios are stated in Table 1.

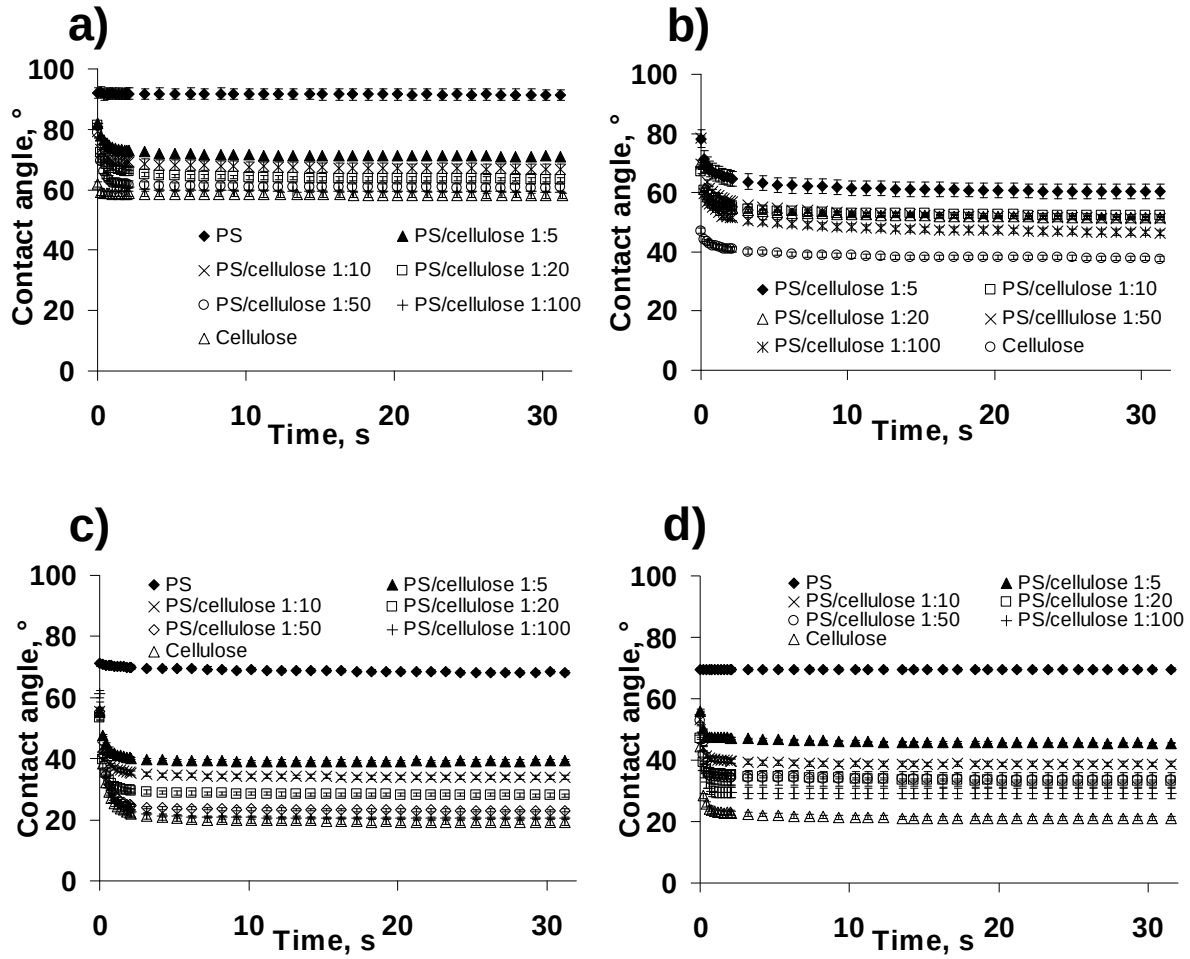

Figure S4. Advancing a) water c) ethylene glycol d) formamide contact angles of the PS/cellulose blend films. b) Advancing water contact angles of the wetted PS/cellulose blend films.

S4 Advancing contact angles with three different probe liquids (water, ethylene glycol and formamide) on PS/cellulose films were measured. Also the effect of wetting and drying the films prior to the measurements was tested. The films are quite stable although some reorientation took place during the first few seconds.